PHYSICAL REVIEW C, VOLUME 61, 031305(R)

Two-frequency shell model for hypernuclei and meson-exchange hyperon-nucleon potentials

Yiharn Tzeng,[1] S. Y. Tsay Tzeng,[2] T. T. S. Kuo,[1,3] T.-S.H. Lee,[4] and V. G. D. Stoks[5]
[1]*Institute of Physics, Academia Sinica, Taipei, Taiwan, Republic of China*
[2] *National Taipei University of Technology, Taipei, Taiwan, Republic of China*
[3]*Department of Physics, State University of New York at Stony Brook, Stony Brook, New York 11794*
[4]*Physics Division, Argonne National Laboratory, Argonne, Illinois 60493*
[5]*Center for the Subatomic Structure of Matter, University of Adelaide, Adelaide, SA5005, Australia*
(Received 29 January 1999; revised manuscript received 28 July 1999; published 18 February 2000)

A two-frequency shell model is proposed for investigating the structure of hypernuclei starting with a hyperon-nucleon potential in free space. In a calculation using the folded-diagram method for $^{16}_{\Lambda}$O, the Λ single particle energy is found to have a saturation minimum at an oscillator frequency $\hbar\omega_\Lambda \approx 10$ MeV, for the Λ orbit, which is considerably smaller than $\hbar\omega_N = 14$ MeV for the nucleon orbit. The spin-dependence parameters derived from the Nijmegen NSC89 and NSC97f potentials are similar, but both are rather different from those obtained with the Jülich-*B* potential. The ΛNN three-body interactions induced by $\Lambda N - \Sigma N$ transitions are important for the spin parameters, but relatively unimportant for the low-lying states of $^{16}_{\Lambda}$O.

PACS number(s): 21.80.+a, 21.60.Cs, 24.10.Cn, 27.20.+n

The shell model has been the main framework for exploring the structure of hypernuclei identified in nuclear reactions induced by pions, kaons, and electromagnetic probes. Its validity was firmly established in experiments [1–3] conducted mainly at the Brookhaven National Laboratory (USA) and KEK (Japan). In an approach based on the many-body theory, it is necessary to develop a reliable method for calculating the effective hyperon-nucleon (YN) interactions in a chosen model space starting with a YN potential in free space. This is needed for using hypernuclei to learn about the YN interactions which are poorly understood mainly because of the lack of extensive YN reaction data.

The calculations of effective YN interactions for shell-model studies have been performed by many authors [4–11]. In almost all of these previous approaches, it was assumed that the harmonic oscillator basis wave functions for nucleons and hyperons are of the same frequency; i.e., $\hbar\omega_\Lambda = \hbar\omega_N$. (For $^{16}_{\Lambda}$O, it is common to use $\hbar\omega_\Lambda = \hbar\omega_N = 11$ MeV.) Dalitz *et al.* [8] have employed higher-nodal oscillator or Woods-Saxon wave functions for the *p*-state lambda particle. In this paper we will demonstrate that a two-frequency shell with $\hbar\omega_\Lambda < \hbar\omega_N$ model is needed to give a more realistic description of the structure of hypernuclei. This is motivated by the following consideration: In shell model descriptions of nuclei, the oscillator frequency $\hbar\omega$ is usually determined by fitting the shell-model nuclear rms radius to the experimental one. The shell-model rms radius is proportional to $1/\sqrt{m\omega}$ where m denotes the baryon mass, and we note that the lambda mass is significantly heavier than the nucleon mass. Thus we see that ω_Λ should be smaller than ω_N if the rms radii for Λ and N are equivalent. Since a Λ hyperon in a nucleus is in general much less bound than nucleons, the rms radius for Λ is likely to be larger than that for N, further suggesting that it may be more appropriate to use different shell-model basis functions for nucleons and hyperons, with $\hbar\omega_\Lambda$ less than $\hbar\omega_N$. This situation is similar to the shell-model approach of halo nuclei. In Ref. [12], it was shown that the use of a different frequency to describe the oscillator wave functions for the halo nucleons is essential in getting a realistic description of the core polarization effects.

Our main framework is based on a folded diagram approach [13–15]. Let us take hypernucleus $^{16}_{\Lambda}$O as an example to illustrate our method. Since the full many-body problem for hypernuclei is usually very difficult to solve in practice, we need to reduce the full-space problem to a manageable problem defined in a model-space P. The equation in the P-space is well known and is formally defined by $(H_0 + V_{eff})P\Psi_m = E_m P\Psi_m$, where the eigenvalues and eigenstates $\{E_m, \Psi_m\}$ belong to a small subset of the solutions of the original full-space many-body Schrödinger equation $H\Psi = E\Psi$. In the above, V_{eff} is the effective interaction, and H_0 is the unperturbed one-body Hamiltonian.

The central problem here is of course to develop a manageable method for calculating the model-space effective interaction V_{eff}, starting from a chosen YN potential V_{YN}. One relatively convenient way is to apply the $\hat{Q}$-box folded-diagram method of Kuo, Lee, and Ratcliff [13,15]. In this way, V_{eff} is given by a $\hat{Q}$-box folded-diagram series, and a first step is to calculate the G matrix by way of the integral equation [10]

$$G(\omega) = V + VQ\frac{1}{\omega - Q(m_N + t_N + m_Y + t_Y)Q}QG(\omega), \qquad (1)$$

where V represents V_{YN} and m and t, respectively, denote the baryon mass and kinetic energy. The Pauli exclusion operator Q is to ensure that the intermediate states in the propagator must be outside the chosen model space P; ω denotes the starting energy.

An exact treatment of the Pauli operator in solving Eq. (1) has been developed [9,10], for the case where the oscillator frequencies for the nucleon and for the hyperon are the same, namely $\hbar\omega_N = \hbar\omega_Y$. We have extended this treatment to the two-frequency case where $\hbar\omega_N$ and $\hbar\omega_Y$ are different. Here we follow closely the methods described in Refs. [9,12], and have employed a Pauli operator specified by $(n_1, n_2, n_3) = (3,10,21)$ for nucleons and $(n_{\Lambda 2}, n_{\Lambda 3}) = (6,10)$ for the lambda particle. In our calculation, we need to perform a laboratory $(n_1 l_1, n_2 l_2)$ to relative and center-of-mass

(nl,NL) transformation for the two-particle shell-model wave function. Here we encounter a well-known technical difficulty, namely a convenient Moshinsky-type theory for performing the above transformation, for the two-frequency case, is not yet available. As was done in Ref. [12], we surmount this difficulty by expanding the wave functions with $\hbar\omega_\Lambda$ in terms of those with $\hbar\omega_N$, or vice versa. Usually it is necessary to include up to eight terms in the expansion to obtain high accuracy.

In this work, the frequency for nucleons is chosen by using the empirical formula $\hbar\omega_N = 45A^{-1/3} - 25A^{-2/3} = 14$ MeV for the considered $A=16$ system. The frequency $\hbar\omega_\Lambda$ for the Λ orbits plays an important role, and is treated as a parameter in our calculation. Clearly the success of this approach depends on whether the predicted ground state energy saturates against the variation of $\hbar\omega_\Lambda$. This may depend critically on the starting baryon-baryon potential V. In this work, we have employed the Nijmegen NSC97 [16] and NSC89 [17] and the Jülich-B [18] YN potentials in our calculation.

We consider the low-lying states of ${}^{16}_{\Lambda}$O to be composed of a Λ particle on one of the $(0s_{1/2},0p_{1/2},0p_{3/2})$ orbits coupled to a neutron-hole on one of the $(0p_{3/2},0p_{1/2})$ orbits. To calculate the spectrum of this hypernucleus, we need to calculate the Λ particle-neutron hole matrix elements of the effective interaction V_{eff}. Following Ref. [11], this is done by first calculating the $\hat{Q}$ box consisting of diagrams first- and second-order in the G matrix. We then sum up the $\hat{Q}$-box folded-diagram series to all orders by using the Lee-Suzuki iteration method [19,20].

We first calculate the single particle (s.p.) energies for the Λ particle with respect to a ^{16}O core by using the above folded-diagram method, with the $\hat{Q}$ box consisting of the one-body diagrams S_1 and S_3 of Ref. [11]. Our results for the Nijmegen potentials are presented in Fig. 1. Here the dependence of the calculated s.p. energies for the $\Lambda s_{1/2}$ orbit on the oscillator frequency $\hbar\omega_\Lambda$ is displayed. The upper curve is obtained with the NSC89 potential. We note that it reaches a saturation minima at $\hbar\omega_\Lambda \approx 10$ MeV which is much smaller than the value $\hbar\omega_N = 14$ MeV for nucleon orbits. The lower curve is obtained with the NSC97f potential, and has a saturation minimum at approximately the same $\hbar\omega_\Lambda$ location.

It should be pointed out that the above calculation deals with the energy difference of two nuclear systems (${}^{17}_{\Lambda}$O and ^{16}O), and it is not a variational calculation in the sense that its saturation minimum is not an upper bound for the exact s.p. energy. However, we should at least require our calculation to be stable with respect to a small variation of $\hbar\omega_\Lambda$, and this requirement is met at the above saturation points. Thus our two-frequency calculation suggests that preferred and reasonable choices for the oscillator frequencies are those given by the above saturation points, namely $\hbar\omega_N = 14$ MeV and $\hbar\omega_\Lambda = 10$ MeV. Consequently, the $\Lambda s_{1/2}$ s.p. energy is given by the energy at the saturation points of these curves, namely -12.6 and -16.9 MeV for the NSC89 and NSC97f potentials, respectively. (The corresponding empirical value is about -12.5 MeV [21].) Fujii, Okamoto, and Suzuki [22] have carried out extensive unitary-model-operator (UMO) calculations for ${}^{17}_{\Lambda}$O using also the Nijmegen potentials. Our results are qualitatively similar to theirs. For example, their UMO results for the above s.p. energy are approximately -11.7 (NSC89) and -16.2 (NSC97f) MeV. We have also tried Nijmegen potentials NSC97a through NSC97e, and obtained similar overbinding for the s.p. energy when using $(\hbar\omega_N,\hbar\omega_\Lambda) = (14,10)$ MeV. In passing, we mention that the above two-frequency s.p. calculation has also been performed using the Jülich-B [18] potential. The shape of the saturation curve obtained is fairly similar to those shown in Fig. 1. The ^{17}O$_\Lambda$ s.p. energy at the saturation point of $\hbar\omega_N = 14$ and $\hbar\omega_\Lambda \approx 10$ MeV is 15.8 MeV, also in satisfactory agreement with the corresponding UMO result of ≈ 15.5 MeV [22].

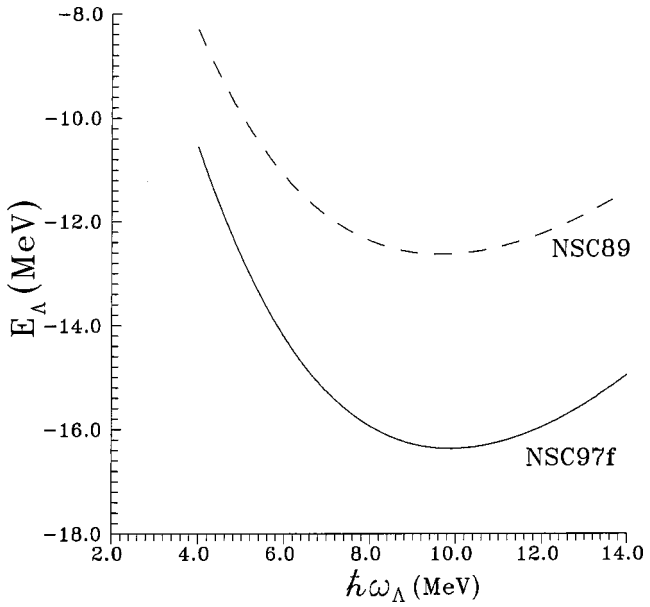

FIG. 1. Dependence of $\Lambda s_{1/2}$ s.p. energies in ${}^{17}_{\Lambda}$O on $\hbar\omega_\Lambda$ obtained from the NSC89 (top curve) and NSC97f (bottom curve) potentials.

As mentioned earlier, one often takes a one-frequency choice with $\hbar\omega_\Lambda = \hbar\omega_N = 11$ MeV in shell model calculation for ${}^{16}_{\Lambda}$O hypernucleus. With this choice the above s.p. energies become -9.9 and -12.7 MeV for the NSC89 and Jülich-B potentials, respectively [11], and -13.1 MeV for the NSC97f potential. Comparing this with the two-frequency calculations, there is a general reduction of the binding energy. A possible reason for this behavior may be the following: When changing $(\hbar\omega_N,\hbar\omega_\Lambda)$ from (14,10) to (11,11) MeV, there are both an increase of the kinetic energy and a decrease of the potential energy, resulting in a net decrease of the s.p. energy.

A possible shortcoming of our present calculation may be pointed out. With $\hbar\omega_N$ fixed at 14 MeV and $\hbar\omega_\Lambda$ approximately in the range of 4 to 14 MeV, our calculated $\Lambda p_{1/2}$ state turns out to be unbound for the NSC89 and NSC97f potentials. Similar unbound behavior was also observed when using the Jülich-B potential for $\hbar\omega_\Lambda$ ranging approximately from 11 to 14 MeV. This state is a very weakly bound state, and the degrees of freedom provided by our

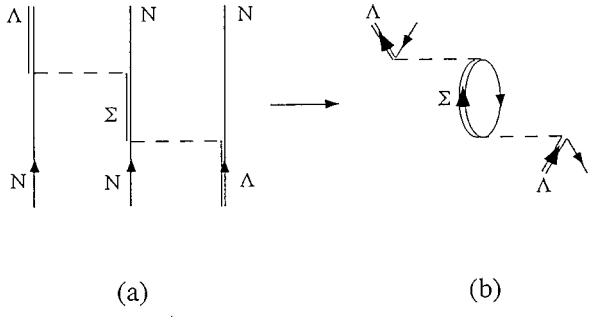

FIG. 2. ΛNN three-body-force diagram in bare vacuum representation (a) and in particle-hole vacuum representation (b).

present model may not be adequate for its description. Further studies of this state within our framework are needed and are being carried out.

Several authors [23,24] have pointed out that the ΛNN three-body force may play an important role for the spin dependence of the ΛN effective interaction. A main purpose of our present work is to study this three-body force, focusing its effect on the low-lying spectrum of $^{16}_{\Lambda}$O and the spin dependence of the ΛN effective interaction. This three-body force is induced by $N\Lambda - N\Sigma$ transitions, as illustrated by diagram (a) of Fig. 2, which is drawn with respect to the bare vacuum. It becomes the particle-hole diagram (b) of the same figure when transformed to the particle-hole vacuum.

In Fig. 3, our results for the spectrum of $^{16}_{\Lambda}$O calculated with the NSC89 and NSC97f potentials are presented. For both calculations, we have used $\hbar\omega_N = 14$ MeV and $\hbar\omega_\Lambda = 10$ MeV. As discussed earlier, at these oscillator frequencies our calculated Λ s.p. energies are found to have saturation minima (stable equilibrium). The columns $2^{\rm nd}-g$ denote the full calculations including all first- and second-order G-matrix diagrams for the $\hat{Q}$ box and the corresponding folded diagrams to all orders. To study the effect of the three-body ΛNN force induced by $N\Lambda - N\Sigma$ transitions, we have repeated the above calculation with the three-body-force diagram (b) of Fig. 2, removed from the calculation. The results are listed in columns No $\Lambda - \Sigma cp$. As seen, the effect of the three-body force on the low-lying spectrum is rather small in general. Its main effect appears to be a raising of the lowest 0^+ state by about 0.3 MeV for the NSC89 case. The spectra given by the NSC89 and NSC97f potentials are both in satisfactory agreement with experiment [21,25].

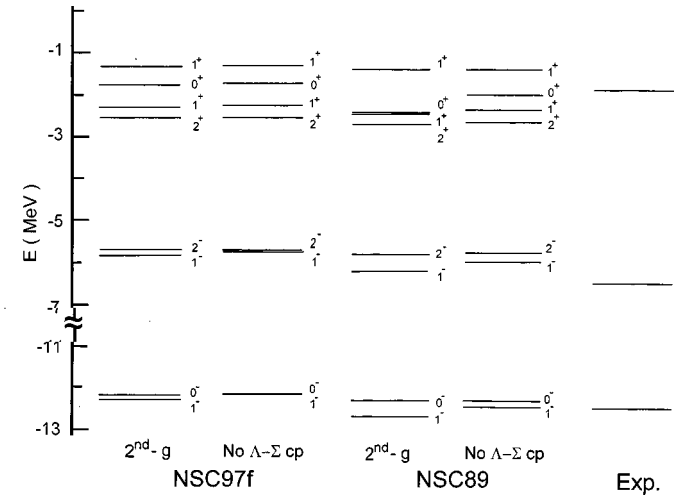

FIG. 3. Enegy spectrum of $^{16}_{\Lambda}$O obtained from the NSC89 and NSC97f potentials.

TABLE I. Central (V), spin-spin (D), Λ spin-orbit (S_Λ), nucleon spin-orbit (S_N), and tensor (T) parameters of the $\Lambda - N$ effective interactions. For each parameter, the results shown in the first, second, and third rows are obtained with the NSC89, NSC97f, and JB potentials, respectively. Oscillator frequencies of $\hbar\omega_N = 14$ and $\hbar\omega_\Lambda = 10$ MeV are used. All entries are in MeV.

Parameter	G_{ph}	$\Lambda\Sigma 3b$	V_{eff}
V	−0.867	0.146	−0.746
	−1.052	0.042	−1.006
	−1.104	0.062	−1.126
D	1.167	0.521	1.540
	0.613	0.154	0.735
	−1.683	0.196	−1.519
S_Λ	−0.267	0.015	−0.272
	−0.143	0.009	−0.163
	−0.025	−0.006	−0.039
S_N	−0.289	0.011	−0.247
	−0.215	0.005	−0.209
	0.004	−0.009	−0.074
T	0.083	0.001	0.083
	0.053	0.000	0.056
	−0.030	−0.003	−0.027

The spin dependence of the $\Lambda - N$ effective interaction has long been an important topic in hypernuclear physics [24,26]. We may generally write the $\Lambda - N$ effective interaction as [26]

$$V_{\Lambda N}(r) = V_o(r) + V_\sigma(r)\mathbf{s_N}\cdot\mathbf{s_\Lambda} + V_\Lambda(r)\mathbf{l_{N\Lambda}}\cdot\mathbf{s_\Lambda} + V_N(r)\mathbf{l_{N\Lambda}}\cdot\mathbf{s_N} + V_T(r)S_{12}. \quad (2)$$

For the $\Lambda s_{1/2}$-$Np_{3/2,1/2}$ interaction, the above effective interaction is completely represented by five parameters: V, D, S_Λ, S_N, and T. They are just certain average radial integrals involving, respectively, the radial potentials V_o, V_σ, V_Λ, V_N, and V_T.

In Table I, we present our results for these five parameters, obtained with the NSC89, NSC97f, and Jülich-B (JB) potentials. In the column, G_{ph} are the spin parameters obtained from the lowest-order particle-hole G-matrix diagram only, without the inclusion of any core polarization diagrams and folded diagrams. As seen, there are significant differences among the parameters given by the Nijmegen and JB potentials, particularly for the parameter D, which represents the strength of the spin-spin interaction V_σ. The values of this parameter given by the Nijmegen and JB potentials are of opposite signs.

In the column, $\Lambda\Sigma 3b$ are the spin parameters given solely by diagram (b) of Fig. 2, namely the ΛNN three-body force

diagram. As seen, this diagram has a strong effect on the parameters V and D for the NSC89 potential, but for the other two potentials the effect is weaker, a reflection that the former has a stronger $\Lambda-\Sigma$ transition potential than the latter. Bodmer and Usmani [23] have investigated s-shell hypernuclei using phenomenological ΛN and ΛNN potentials. They found that the contribution to the spin dependence from their ΛNN three-body force reduces that from their ΛN force by $\approx 1/3$. This behavior is not observed for our results, as seen from Table I. For instance, the spin parameter D given by our ΛN G matrix is enhanced by $\approx 1/2$ by our ΛNN force for the NSC89 case.

The last column of Table I lists the parameters obtained with the V_{eff} matrix elements, with the inclusion of both core polarization and folded diagrams. Generally speaking, the tensor and spin-orbit components of all three potentials are weak. The central component of the JB potential is the strongest among the three potentials considered. The spin-spin component of the JB potential is large and of opposite sign from the other two.

In summary, we have developed a two-frequency shell model for investigating hypernuclei starting with a meson-exchange YN potential. In a hypernucleus, hyperons are generally less bound than nucleons, the former being more spatially extended. With this consideration in mind, we have allowed the oscillator frequency for the hyperon to be different from that for the nucleon wave function. We have applied this approach to a folded-diagram G-matrix calculation of ${}^{16}_{\Lambda}$O. The validity of this approach is supported by our results that the predicted Λ s.p. energy exhibits a saturation minimum at $\hbar\omega_\Lambda \approx 10$ MeV which is much smaller than the value $\hbar\omega_N = 14$ MeV for nucleons. The $\Lambda s_{1/2}$ s.p. energies given by the NSC97 potentials are about 3 MeV more than that by the NSC89 potential, in qualitative agreement with the UMO results of Fujii *et al.* [22].

Using our two-frequency shell model, we have calculated the spin-dependence parameters for the $\Lambda-N$ effective interactions. Our results show that the ΛNN three-body interaction calculated from the NSC89 potential has a large effect on the spin parameters. The predicted energies for the low-lying states of ${}^{16}_{\Lambda}$O are generally close to the experimental values, and are not significantly affected by the ΛNN three-body force. A central parameter in our approach is the oscillator frequency $\hbar\omega_\Lambda$ for the Λ orbits. The rms radius for the Λ particle is directly related to $\hbar\omega_\Lambda$. Although it may be difficult to measure this radius experimentally, such a measurement would certainly be very helpful in putting a strict constraint on the $\hbar\omega_\Lambda$ value.

We believe that the two-frequency shell-model approach provides a more realistic framework than the conventional (one-frequency) shell-model approach for understanding the structure of hypernuclear nuclei in terms of the elementary YN interactions. It will be very useful in probing the hypernuclear dynamics using the new data from the Thomas Jefferson Laboratory as well as other new hadron facilities.

This work was supported partly by NSC (Taiwan) Grant NSC87-2112-M-001-004Y, U.S. NSF Grant No. INT9601361, U.S. DOE Grant No. DE-FG02-88ER0388, and U.S. DOE Nuclear Physics Division Contract No. W-31-109-ENG-38.

[1] R. E. Chrien, Nucl. Phys. **A478**, 705c (1988).
[2] P. H. Pile *et al.*, Phys. Rev. Lett. **66**, 2585 (1991).
[3] T. Hasegawa *et al.*, Phys. Rev. C **53**, 1210 (1996).
[4] Y. Yamamato, H. Bandō, and J. Žofka, Prog. Phys. **80**, 757 (1988).
[5] T. Motoba, H. Bandō, R. Wünsch, J. Žofka, Phys. Rev. C **38**, 1322 (1988).
[6] Y. Yamamoto and H. Bandō, Prog. Theor. Phys. **73**, 905 (1985); H. Bandō, T. Motoba, and J. Žofka, Int. J. Mod. Phys. A **5**, 4021 (1990).
[7] T. Motoba, Nucl. Phys. **A639**, 135c (1998).
[8] D. H. Dalitz, D. H. Davis, T. Motoba, and D. N. Tovee, Nucl. Phys. **A625**, 71 (1997).
[9] Jifa Hao, T. T. S. Kuo, A. Reuber, K. Holinde, J. Speth, and D. J. Millener, Phys. Rev. Lett. **71**, 1498 (1993).
[10] T. T. S. Kuo and Jifa Hao, Prog. Theor. Phys. Suppl. **117**, 351 (1994).
[11] Yiharn Tzeng, S. Y. Tsay Tzeng, T. T. S. Kuo, and T.-S. H. Lee, Nucl. Phys. **A639**, 165c (1998); Phys. Rev. C **60**, 044305 (1999).
[12] T. T. S. Kuo, F. Krmpotic, and Y. Tzeng, Phys. Rev. Lett. **78**, 2708 (1997).
[13] T. T. S. Kuo and E. Osnes, *Springer Lecture Notes in Physics* Vol. 364, 1 (1990), p. 1.
[14] P. J. Ellis and E. Osnes, Rev. Mod. Phys. **49**, 777 (1977).
[15] T. T. S. Kuo, S. Y. Lee, and K. F. Ratcliff, Nucl. Phys. **A176**, 65 (1971).
[16] T. A. Rijken, V. G. J. Stoks, and Y. Yamamoto, Phys. Rev. C **59**, 21 (1997).
[17] P. M. M. Maessen, T. A. Rijken, and J. J. de Swart, Phys. Rev. C **40**, 2226 (1989).
[18] B. Holzenkamp, K. Holinde, and J. Speth, Nucl. Phys. **A500**, 485 (1989).
[19] S. Y. Lee and K. Suzuki, Phys. Lett. **91B**, 173 (1980).
[20] K. Suzuki and S. Y. Lee, Prog. Theor. Phys. **64**, 2091 (1980).
[21] H. Tamura, R. S. Hayano, H. Outa, and T. Yamazaki, Prog. Theor. Phys. Suppl. **117**, 1 (1994).
[22] S. Fujii, R. Okamoto, and K. Suzuki, in *Proceedings of the Strangeness Nuclear Physics (SNP'99) Workshop*, Seoul, Korea, 1999 (World Scientific, Singapore, to be published).
[23] A. R. Bodmer and Q. N. Usmani, Nucl. Phys. **A477**, 621 (1988), and references therein.
[24] A. Gal, in *Plots, Quarks and Strange Particles*, Proceedings of the Dalitz Conference 1990, edited by I. J. R. Aitchison, C. H. Llewellyn Smith, and J. E. Paton (World Scientific, Singapore, 1990).
[25] O. Hashimoto, Nucl. Phys. **A639**, 93c (1998).
[26] D. J. Millener, A. Gal, C. B. Dover, and R. H. Dalitz, Phys. Rev. C **31**, 499 (1985).